Received February 16, 2017, accepted March 12, 2017, date of publication April 24, 2017, date of current version June 7, 2017.

Digital Object Identifier 10.1109/ACCESS.2017.2692245

Semisoft Generalized Total Variation Minimization for Image Reconstruction in Computed Tomography

XIEZHANG LI[1], FANGJUN ARROYO[2], JIEHUA ZHU[1], AND JIANING SUN[3]

[1]Department of Mathematical Sciences, Georgia Southern University, Statesboro, GA 30460 USA
[2]Department of Mathematics, Francis Marion University, Florence, SC 29501 USA
[3]School of mathematics, Northeast Normal University, Changchun, China

Corresponding author: Jiehua Zhu (jzhu@georgiasouthern.edu)

The work of X. Li and J. Zhu was supported by the Office of Research Services and Sponsored Programs at Georgia Southern University.

ABSTRACT The generalized l_1 greedy algorithm was recently proposed and shown to outperform the standard reweighted l_1-minimization and l_1-greedy algorithms for image reconstruction in computed tomography (CT). Herein, this algorithm is extended as a semisoft generalized l_1 greedy algorithm by adapting the wavelet technique of semisoft thresholding. The extended algorithm can also be applied to image reconstruction by incorporating it into the BCPCS framework, resulting in a semisoft generalized total variation minimization (SSGTV) algorithm for CT. Numerical tests indicate that the proposed SSGTV algorithm improves the image reconstruction for CT.

INDEX TERMS Generalized l_1 greedy algorithm, reweighted l_1-minimization, semisoft thresholding, total variation.

I. INTRODUCTION

Iterative algebraic algorithms are widely applied in signal processing and image reconstruction since they yield more accurate results than analytic approaches in certain cases. Let

$$Ax = b \tag{1}$$

be a consistent underdetermined system of linear equations, where A is an $m \times n$ matrix ($m \ll n$), $x \in \mathbb{R}^n$ a sparse signal vector and $b \in \mathbb{R}^m$ the measurement vector. Finding the sparsest solution of the system is equivalent to solving the following l_0 -minimization problem

$$\min ||x||_0 \quad \text{subject to } Ax = b.$$

However, the l_0-minimization problem is NP-hard [15]. Compressed sensing theory suggests an alternative l_1-minimization

$$\min \|x\|_1 \quad \text{subject to } Ax = b, \tag{2}$$

to recover sparse signals x [5], [8]. However, l_1-minimization is biased against sparse signals with a few large components. To address this setback the standard reweighted l_1-minimization algorithm [6] minimizes $\|W^k x\|_1$ instead of $\|x\|_1$, where $W^k = \operatorname{diag}\{w_1^k, \cdots, w_n^k\}$ with w_i^k, $1 \le i \le n$, inversely proportional to the magnitude of x_i^{k-1}, i.e.,

$$w_i^k = \frac{1}{\varepsilon + \left|x_i^{k-1}\right|}.$$

Here $\varepsilon > 0$ is chosen to avoid division by zero.

The above weights were modified in the l_1 greedy algorithm [16] as

$$w_i^k = \begin{cases} \delta, & \text{for } \left|x_i^{k-1}\right| \ge \beta^k M \\ 1, & \text{otherwise,} \end{cases}$$

where β is a parameter between 0 and 1, and $M = \|x^0\|_\infty$ for an initial solution x^0. Later the weights were further extended as

$$w_i^k = \begin{cases} \delta, & \text{for } \left|x_i^{k-1}\right| \ge \beta M s^{k-1} \\ \gamma, & \text{for } \left|x_i^{k-1}\right| < \alpha M s^{k-1} \\ \dfrac{1}{\varepsilon + \left|x_i^{k-1}\right|}, & \text{otherwise,} \end{cases} \tag{3}$$

where $0 \le \alpha \le \beta \le 1$, $\gamma \ge 1000$, $\delta \in (0, \frac{1}{1000}]$, $s \in (0, 1]$, $\varepsilon > 0$, in the generalized l_1 greedy (GLG) algorithm [19].

2169-3536 © 2017 IEEE. Translations and content mining are permitted for academic research only.
Personal use is also permitted, but republication/redistribution requires IEEE permission.
See http://www.ieee.org/publications_standards/publications/rights/index.html for more information.

Algorithm 1 Generalized l_1 Greedy Algorithm (GLG)

1. generate x^0 by reweighted l_1-minimization.
2. set $M = ||x^0||_\infty$, initialize parameters.
3. for $k = 1$ to $k_{\max}$
   3.1. update the diagonal matrix W^k by (3).
   3.2. solve the reweighted l_1-minimization problem:
   $x^k = \arg\min ||W^k x||_1 \quad$ subject to $\quad Ax = b$.
   3.3. return if a stop criterion holds.
   end

In [19], the GLG algorithm was applied to computed tomography (CT) image recovery. The details are discussed below after introducing some terminology and notations.

In computed tomography (CT), the gradients of images are often sparse because most images can be approximately modeled to be essentially piecewise constant. So a 2D image x in CT can be effectively reconstructed by minimizing the following total variation [4], [6],

$$\min ||x||_{TV} \quad \text{subject to } Ax = b, \tag{4}$$

where the total variation $||x||_{TV}$ is defined as the l_1 -norm of the magnitudes of the components of the discrete gradient,

$$||x||_{TV} = \sum\nolimits_{i,j} \sqrt{(x_{i+1,j} - x_{i,j})^2 + (x_{i,j+1} - x_{i,j})^2},$$

and the symbol x in the system $Ax = b$ stands for the vector corresponding to the 2D image x for convenience.

Let a^i and b_i be the ith column of A^T and the ith component of b, respectively. The orthogonal projection from x to the ith hyperplane $H_i = \{y : \langle y, x\rangle = b_i\}$, where $\langle y, x\rangle$ is the inner product, is given by

$$P_i x = x + \frac{b_i - \langle a^i, x\rangle}{||a^i||_2^2} a^i.$$

A cyclic projection is a composition of the projections to each hyperplane H_i, $i = 1, 2, \ldots, n$. Suppose that A and b in the system (1) are partitioned, respectively, as

$$A = \begin{bmatrix} A_1 \\ \vdots \\ A_r \end{bmatrix} \text{ and } b = \begin{bmatrix} b^1 \\ \vdots \\ b^r \end{bmatrix},$$

where the jth block corresponds to the jth projection direction for $j = 1, 2, \ldots, r$.

A block cyclic projection method incorporating the total variation minimization in the compressed sensing scheme (BCPCS) was introduced in [14] and its convergence was derived in [2], [3]. The BCPCS algorithm is performed as follows: for each block, first a cyclic projection is applied and then an approximation x is updated by the steepest decent method. Let μ be the gradient of x. The steepest decent direction d is computed by $d = -\frac{\partial}{\partial x}\sum|\mu|$. An approximation x is updated by $x = x + \tau d/||d||_\infty$ with a step size τ. Repetition of the procedure will solve the total variation minimization.

As an application of the GLG algorithm, the generalized total variation minimization (GTV) algorithm below incorporates the GLG algorithm into the BCPCS framework to recover CT images [19].

Algorithm 2 Generalized Total Variation Minimization for CT (GTV)

1. generate x^0 by reweighted l_1-minimization.
2. initialize parameters.
3. for $k = 1$ to $k_{\max}$
   for $j = 1$ to r
   3.1. update x^{k-1} using a cyclic projection on the jth block.
   3.2. calculate the gradient μ of x^{k-1} and the steepest decent direction d.
   3.3. revise weights w_i^k by (3).
   3.4. set a reweighted direction $d = W^k d$.
   3.5. update $x^{k-1} = x^{k-1} + \tau_k \frac{d}{||d||_\infty}$, $\sum \tau_k < \infty$.
   end
   3.6. $x^k = x^{k-1}$.
   end

Numerical tests have shown that the GLG and GTV algorithms outperform both the reweighted l_1-minimization and l_1 greedy algorithms in signal recovery and CT image reconstruction [1]. However, the discontinuity of the weight functions used in these algorithms is likely to generate artifacts which affect the accuracy of the results. In this paper, we address these shortcomings by modifying the weight function making use of the concept of thresholding from the wavelet literature.

The rest of this paper is organized as follows. In Section II, a semisoft generalized l_1 greedy (SSGLG) algorithm is proposed and then incorporated into the BCPCS framework to develop a semisoft generalized total variation minimization (SSGTV) algorithm for CT. Numerical tests of the algorithm in reconstructing medical images are conducted and the results are reported in Section III. Final conclusions are drawn in Section IV.

II. SSGLG AND SSGTV ALGORITHMS

In this section, we will improve the GLG algorithm by adapting the wavelet technique of semisoft thresholding.

Wavelet thresholding techniques have been used to improve the performance of wavelet transformations in signal processing and speech enhancement [7], [9]. There are three common thresholdings: hard, soft, and semisoft thresholdings. They are defined as follows. For a certain positive threshold t and positive thresholds $t_1 < t_2$,

(i) hard thresholding:

$$h_1(x) = \begin{cases} x, & \text{if } |x| > t \\ 0, & \text{if } |x| \le t \end{cases}$$

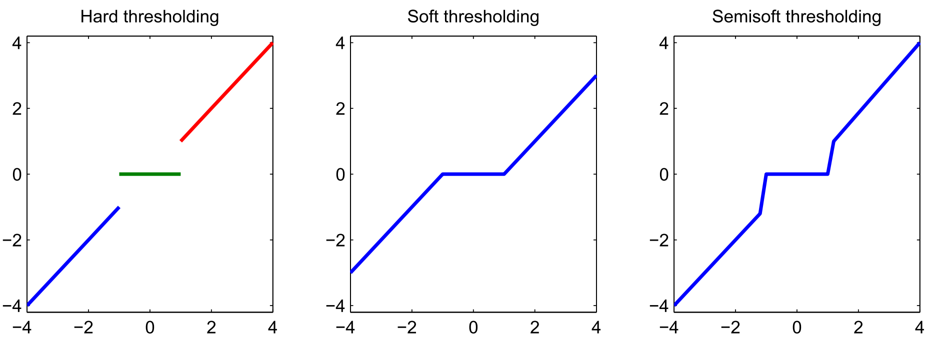

FIGURE 1. Three common thresholdings.

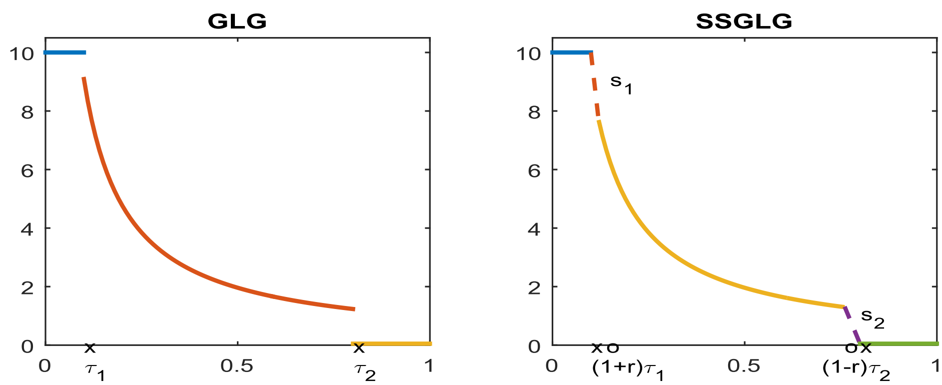

FIGURE 2. The weights for GLG and SSGLG algorithms.

(ii) soft thresholding:

$$h_2(x) = \begin{cases} \text{sign}(x)(|x| - t), & \text{if } |x| > t \\ 0, & \text{if } |x| \le t \end{cases}$$

(iii) semisoft thresholding:

$$h_3(x) = \begin{cases} 0, & \text{if } |x| \le t_1 \\ \text{sign}(x)\dfrac{t_2(|x| - t_1)}{t_2 - t_1}, & \text{if } t_1 < |x| \le t_2 \\ x, & \text{if } |x| > t_2 \end{cases}$$

The graphs of the three thresholding functions are shown in Figure 1. The hard thresholding function causes discontinuity of the wavelet coefficients of a signal and possibly generates artifacts. But soft thresholding, though keeping smoother coefficients, affects the accuracy of the reconstructed signal because of the constant deviation between the true and estimated signals. The semisoft thresholding function overcomes the disadvantages of the hard and soft thresholdings with respect to the output quality [11], [17]. In this paper, semisoft thresholding is implemented in the weight function of the GTV algorithm to improve its performance.

Observe that the weight function (3) in the k-th iteration of the GLG algorithm assigns a very large weight γ for entries with magnitudes smaller than $\tau_1 = \alpha M s^{k-1}$, a very small weight δ for entries with magnitudes greater than $\tau_2 = \beta M s^{k-1}$, and reciprocal weight $\frac{1}{\varepsilon + |x_i^{k-1}|}$ for the remaining entries. The discontinuity of the weight function can be seen in Figure 2. With the technique of semisoft threshold, the new algorithm makes use of a continuous weight function as follows.

In the new algorithm, a parameter $r \in (0, 0.1]$ is introduced to shrink the domain of the reciprocal curve to $[(1 + r)\tau_1, (1 - r)\tau_2]$. Two line segments $s_1(x)$ and $s_2(x)$ are utilized on the intervals $[\tau_1, (1 + r)\tau_1]$ and $[(1 - r)\tau_2, \tau_2]$ to connect the reciprocal curve with the constant levels $w = \gamma$, $w = \delta$, respectively. As a consequence, the new weight function is continuous without a constant deviation, as shown in Figure 2. More precisely, the weights w_i^k in the k-th iteration of the proposed semisoft generalized l_1 greedy (SSGLG) algorithm for signal recovery are revised by

$$w_i^k = \begin{cases} \gamma, & \text{for } \left|x_i^{k-1}\right| < \tau_1 \\ s_1(x_i^{k-1}), & \text{for } \tau_1 \le \left|x_i^{k-1}\right| \le (1+r)\tau_1 \\ \dfrac{1}{\varepsilon + |x_i^{k-1}|}, & \text{for } (1+r)\tau_1 < \left|x_i^{k-1}\right| < (1-r)\tau_2 \\ s_2(x_i^{k-1}), & \text{for } (1-r)\tau_2 \le \left|x_i^{k-1}\right| \le \tau_2 \\ \delta, & \text{for } \left|x_i^{k-1}\right| > \tau_2. \end{cases} \tag{5}$$

It is remarked that the weight function in (5) is an extension of the one used in the GLG algorithm. As r approaches 0,

Algorithm 3 Semisoft Generalized l_1 Greedy (SSGLG) Algorithm

1. initialize x^0 by reweighted l_1-minimization.
2. Initialize parameters.
3. for $k = 1$ to $k_{\max}$
    3.1. update weights in W^k using (5).
    3.2. $x^k = \arg\min_x ||W^k x||_1$ subject to $Ax = b$.

   end

the new weight function is reduced to the one in the GLG algorithm.

The SSGLG algorithm can also be applied to image reconstruction by incorporating it into the BCPCS framework, resulting in the following new algorithm.

Algorithm 4 Semisoft Generalized Total Variation Minimization (SSGTV) for CT

1. initialize x^0 by reweighted l_1-minimization.
2. initialize parameters.
3. for $k = 1$ to $k_{\max}$
   for each block of A
    3.1.update x^{k-1} using a cyclic projection.
    3.2.compute gradient μ, steepest decent direction d.
    3.3.update $d = W^k d$ using (5).
    3.4.update $x^{k-1} = x^{k-1} + t_k \frac{d}{||d||_\infty}$, $\sum t_k < \infty$.
   end
   3.5. $x^k = x^{k-1}$.
   3.6. exit if a stop criterion holds.

   end

III. NUMERICAL TESTS

The SSGTV algorithm is tested with the 2D Shepp-Logan phantom [10] and a CT cardiac image [18] of size 256×256 to compare its performance with the standard total variation minimization (TV) (4) and the GTV algorithms. All tests are conducted for the three reconstruction algorithms under the same parameters on an Intel i7 3.40 GHz PC with MATLAB.

The strip-based projection model [13], [20] takes into account x-ray beams of finite width. The projection equations are defined to be the sum of fractional areas of the cells covered by the x-ray beams. Therefore, the strip-based projection model is closer to reality than the line-based projection model in some applications. It is implemented using rational slope projections in order to generate a consistent and underdetermined system $Ax = b$, where A is a sparse 0-1 block matrix, x is the reconstruction image, and b is the projection data. The number of blocks of A is the same as the number of projection directions used, i.e., each block of A corresponds to a rational projection direction. The location of the unique entry of value one in every column within each block is well determined [12]. For example, let C be the 0-1 sub-matrix of A with N^2 columns generated from scanning an N-by-N image along a rational direction $-p/q$, where the integers $p, q > 0$ and $\gcd(p, q) = 1$. Then the entry $c_{ij} = 1$ if and only if $i = pu + qv + 1$ and $j = uN + v + 1$ for some nonnegative integers $u, v < N$. Thus for the ith row of C there are at most N entries of value 1, whose column indices are known and denoted by a set J_i. The ith component of the product Cx is equal to $\sum_{j \in J_i} x_j$. In other words, the vector multiplication of matrices is implemented in terms of scalar addition operations to significantly reduce the computational cost.

The values of the parameters in the GTV and SSGTV algorithms are listed below:

$$\alpha = 0.13, \quad \beta = 0.8, \ \gamma = 1000,$$
$$\delta = 0.001, \quad \varepsilon = 0.1, \ s = 0.9, \ t_k = 0.7 \times 0.97^{k-1}.$$

An additional parameter $r = 0.05$ is used in the SSGTV algorithm.

The total iteration number is preset to 100 for all the algorithms. For the GTV and SSGTV algorithms, 5 iterations of the standard total variation minimization and 20 iterations of the reweighted l_1-minimization are set to yield an initial solution x^0. The parameter $k_{\max}$ for the maximum number iterations in Step 3 of both algorithms is set to 75.

Let G denote a reconstructed image of a 2D image f and f_{ave} denote the average of the pixel values of f. The relative error $RE = \frac{\|f-G\|_2}{\|f\|_2} < 0.005$ is selected as an alternative stop criterion for both GTV and SSGTV iterations.

Experimental results are also evaluated using the root-mean-square error (RMSE), the normalized root mean square deviation (NRMSD), and the normalized mean absolute deviation (NMAD) which are defined as follows:

$$RMSE = \sqrt{\frac{\sum_{m,n}(f(m,n) - G(m,n))^2}{m * n}},$$
$$NRMSD = \sqrt{\frac{\sum_{m,n}(f(m,n) - G(m,n))^2}{\sum_{m,n}(f_{ave} - f(m,n))^2}},$$
$$NMAD = \frac{\sum_{m,n} |f(m,n) - G(m,n)|}{\sum_{m,n} |f(m,n)|}.$$

These measurements reflect different aspects of the quality of the recovered images. RMSE evaluates the reconstruction quality on a pixel-by-pixel basis. NRMSD emphasizes large errors in a few pixels of the recovered image. NMAD focuses on small errors in the recovered image.

In our tests with the Shepp-Logan phantom, the strip-based model is implemented with projections in 24 different directions. The size of the resulting coefficient matrix A is 26002×65536. The reconstructed images are shown in the first row of Figures 3. The experimental results are summarized in Table 1. From Table 1 one can easily determine that the values of RE, RMSE, NRMSD, and NMAD for the SSGTV algorithm are 87%, 91%, 87%, and 97%, respectively, smaller than the corresponding values for the

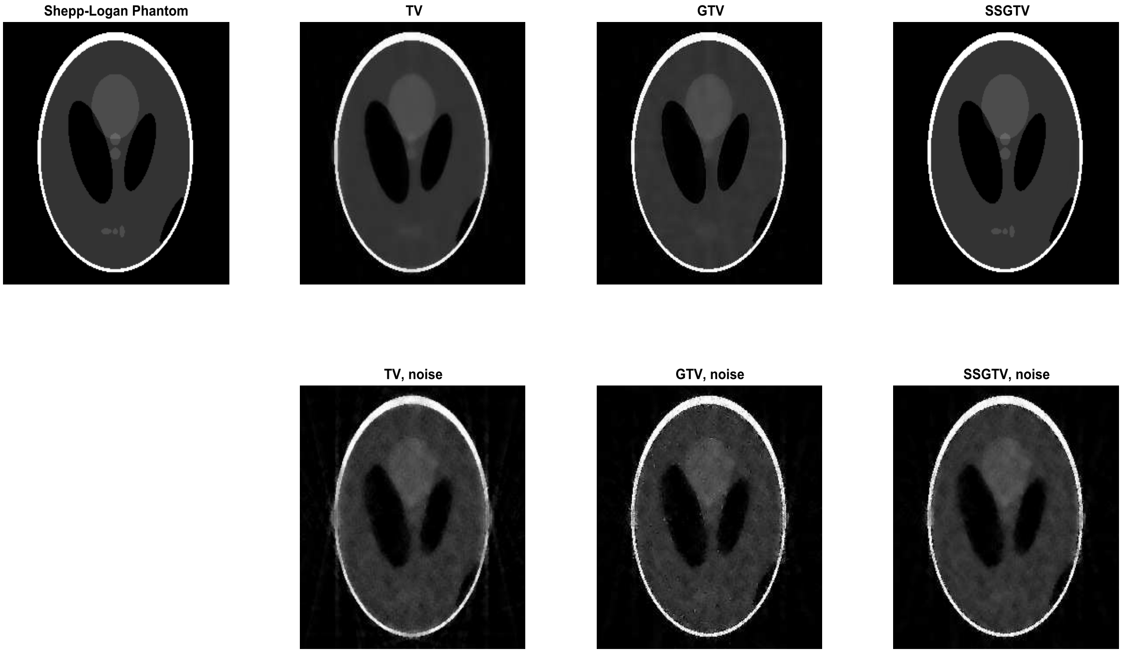

FIGURE 3. Shepp-Logan phantom and reconstructed images.

TABLE 1. Experimental data with Shepp-Logan phantom.

Algorithm	Number of iterations	Time	RE	RMSE	NRMSD	NMAD
TV	100 l_1 min	29.1 sec	0.110	0.027	0.127	0.091
GTV	5 l_1 min + 20 rew + 75 gtv	31.5 sec	0.046	0.011	0.053	0.058
SSGTV	5 l_1 min + 20 rew + 75 ssgtv	32.3 sec	0.006	0.001	0.007	0.002

TABLE 2. Experimental data with a cardiac image.

Algorithm	Number of iterations	Time	RE	RMSE	NRMSD	NMAD
TV	100 l_1 min	41.0 sec	0.108	0.039	0.128	0.114
GTV	5 l_1 min + 20 rew + 75 gtv	44.9 sec	0.035	0.013	0.042	0.040
SSGTV	5 l_1 min + 20 rew + 75 ssgtv	46.7 sec	0.017	0.006	0.020	0.016

TABLE 3. Experimental data with Shepp-Logan phantom in noisy projection.

Algorithm	Number of iterations	Time	RE	RMSE	NRMSD	NMAD
TV	45 l_1 min	10.1 sec	0.280	0.069	0.322	0.298
GTV	5 l_1 min + 10 rew + 30 gtv	10.3 sec	0.251	0.062	0.289	0.254
SSGTV	5 l_1 min + 10 rew + 30 ssgtv	10.6 sec	0.227	0.056	0.261	0.218

GTV algorithm. Table 1 also shows that the GTV algorithm produces more large errors in a few pixels and more small errors in many pixels than the SSGTV algorithm, demonstrating the better performance of SSGTV.

The graph of relative errors vs. the number of iterations for the three different algorithms appears in Figure 4 (a). It is observed that during the last 47 iterations the relative error RE for the SSGTV algorithm is reduced from 0.046 to 0.006 while RE for the GTV algorithm changes only slightly and slowly from 0.0611 to 0.046 and remains the same afterwards. In summary, the SSGTV algorithm applied to the Shepp-Logan phantom results in significant improvements in all the measurements (RE, RMSE, NRMSD, and NMAD) compared with the GTV algorithm with comparable times.

Tests are also conducted with a real CT cardiac image to compare the performance of the algorithms. The CT cardiac image is preprocessed to produce the desired sparsity. For this test 32 directions are chosen in the implementation of the strip-based model. The size of the resulting coefficient matrix A is 39254×65536. The reconstructed images are shown in Figure 5. The experimental results are summarized in Table 2, and the corresponding relative errors are shown

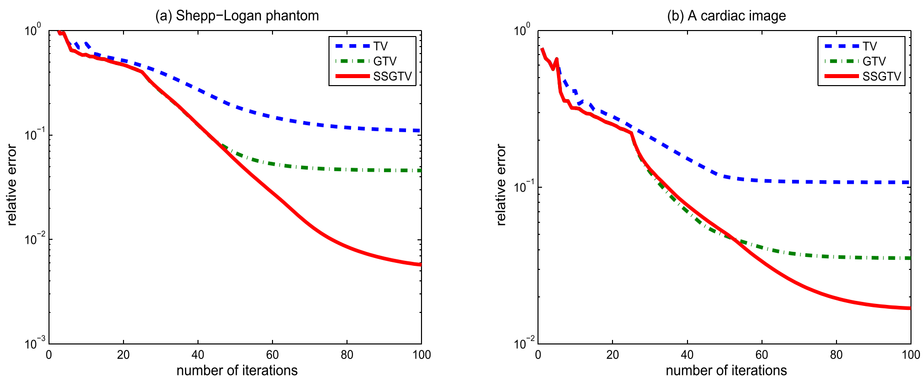

FIGURE 4. Relative errors of reconstruction: (a) Shepp-Logan phantom; (b) cardiac image.

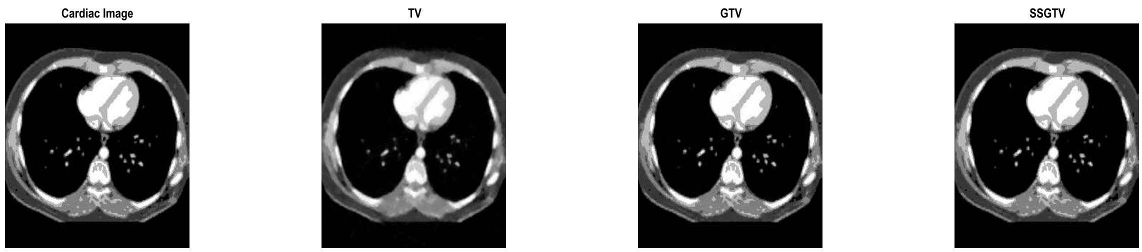

FIGURE 5. Cardiac image and reconstructed images.

in Figure 4 (b). The numerical results indicate again that the SSGTV algorithm is superior to the other two algorithms in image recovery in CT.

To evaluate the performance of SSGTV for the Shepp-Logan phantom with noisy data, Gaussian noise with standard deviation of 0.04 was added to synthetic projection data. The total iteration number is preset to 45, and the values of some parameters are slightly adjusted. The reconstructed images are shown in the second row of Figure 3, and the experimental data are summarized in Table 3. The results also indicate the improvement of SSGTV over GTV but to a smaller extent than with the non-noisy data.

IV. CONCLUSION

The generalized l_1 greedy (GLG) algorithm has recently been developed to solve an underdetermined linear system $Ax = b$ for a sparse solution. However, the weight function in the GLG algorithm is discontinuous and thus affects the accuracy of a solution. In this paper, the GLG algorithm is extended as a semisoft generalized l_1 greedy (SSGLG) algorithm with a continuous weight function utilizing the technique of wavelet semisoft thresholding. The SSGLG algorithm is applied to image reconstruction in CT resulting in a semisoft generalized total variation minimization (SSGTV) algorithm and implemented in the block cyclic projection method in the compressed sensing scheme.

In image reconstruction experiments, the relative error (RE), the root-mean-square error (RMSE), the normalized root mean square deviation (NRMSD), and the normalized mean absolute deviation (NMAD) are used to measure the quality of recovered images. Numerical tests on the Shepp-Logan phantom and a CT cardiac image demonstrate that for all these metrics the SSGTV algorithm outperforms the standard total variation and generalized total variation algorithms in image recovery in the noise-free case. In the tests, the selections of the values of the parameters for the SSGTV algorithm are not optimal. However, numerical experiments indicate that the advantages of the SSGTV algorithm are not affected by different values of the parameters involved. The optimal selections of parameters for the SSGTV will be investigated in the future.

The performance of the SSGTV algorithm with noisy images will be further studied taking into consideration neighboring pixel correlations.

REFERENCES

[1] F. Arroyo, E. Arroyo, J. Zhu, and X. Li, "Numerical studies of the generalized L_1 greedy algorithm for sparse signals," *Adv. Comput. Tomogr.*, vol. 2, pp. 132–139, Dec. 2013.

[2] F. Arroyo, E. Arroyo, X. Li, and J. Zhu, "The convergence of block cyclic projection with underrelaxation parameters for compressed sensing based tomography," *J. X-Ray Sci. Technol.*, vol. 22, no. 2, pp. 197–211, Jan. 2014.

[3] F. Arroyo, E. Arroyo, X. Li, and J. Zhu, "The convergence of the block cyclic projection with an overrelaxation parameter for compressed sensing based tomography," *J. Comput. Appl. Math.*, vol. 280, pp. 59–67, May 2015.

[4] P. Blomgren and T. F. Chan, "Color TV: Total variation methods for restoration of vector-valued images," *IEEE Trans. Image Process.*, vol. 7, no. 3, pp. 304–309, Mar. 1998.

[5] E. J. Candes and T. Tao, "Near-optimal signal recovery from random projections: Universal encoding strategies?" *IEEE Trans. Inf. Theory*, vol. 52, no. 12, pp. 5406–5425, Dec. 2006.

[6] E. J. Candès, M. B. Wakin, and S. P. Boyd, "Enhancing sparsity by reweighted ℓ_1 minimization," *J. Fourier Anal. Appl.*, vol. 14, nos. 5–6, pp. 877–905, 2008.

[7] D. L. Donoho, "De-noising by soft-thresholding," *IEEE Trans. Inf. Theory*, vol. 41, no. 3, pp. 613–627, May 1995.

[8] D. L. Donoho, "Compressed sensing," *IEEE Trans. Inf. Theory*, vol. 52, no. 4, pp. 1289–1306, Apr. 2006.

[9] D. L. Donoho and J. M. Johnstone, "Ideal spatial adaptation by wavelet shrinkage," *Biometrika*, vol. 81, no. 3, pp. 425–455, 1994.

[10] A. C. Kak and M. Slaney, *Principles of Computerized Tomographic Imaging*. Philadelphia, PA, USA: SIAM, 2001.

[11] S. Liu, Y. Li, X. Hu, L. Liu, and D. Hao, "A novel thresholding method in removing noises of electrocardiogram based on wavelet transform," *J. Inf. Comput. Sci.*, vol. 10, no. 15, pp. 5031–5041, 2013.

[12] X. Li, H. Wang, Y. Wu, and J. Zhu, "A full row-rank system matrix generated along two directions in discrete tomography," *Appl. Math. Comput.*, vol. 218, no. 1, pp. 107–114, Sep. 2011.

[13] X. Li and J. Zhu, "A note of reconstruction algorithm of the strip-based projection model for discrete tomography," *J. X-Ray Sci. Technol.*, vol. 16, no. 4, pp. 253–260, Jan. 2008.

[14] X. Li and J. Zhu, "Convergence of block cyclic projection and Cimmino algorithms for compressed sensing based tomography," *J. X-Ray Sci. Technol.*, vol. 18, no. 4, pp. 369–379, Aug. 2010.

[15] B. Natarajan, "Sparse approximate solutions to linear systems," *SIAM J. Comput.*, vol. 24, no. 2, pp. 227–234, Apr. 1995.

[16] A. Petukhov and I. Kozlov, "Fast implementation of l^1 greedy algorithm," *Recent Adv. Harmon. Anal. Appl.*, vol. 25. pp. 317–326, 2012.

[17] T. Sanam and C. Shahnaz, "A combination of semisoft and μ-law thresholding functions for enhancing noisy speech in wavelet packet domain," in *Proc. 7th IEEE Int. Conf. Elect. Comput. Eng. (ICECE)*, Dec. 2012, pp. 20–22.

[18] *TEAM RADS*. [Online]. Available: http://teamrads.com/.

[19] J. Zhu and X. Li, "A generalized ℓ_1 greedy algorithm for image reconstruction in CT," *Appl. Math. Comput.*, vol. 219, no. 10, pp. 5487–5494, Jan. 2013.

[20] J. Zhu, X. Li, Y. Ye, and G. Wang, "Analysis on the strip-based projection model for discrete tomography," *Discrete Appl. Math.*, vol. 156, no. 12, pp. 2359–2367, Jun. 2008.

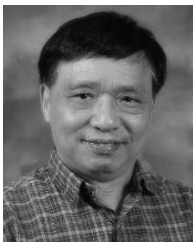

XIEZHANG LI received the Ph.D. degree in applied mathematics from Kent State University, Kent, OH, USA, in 1990. He is currently a Professor of Mathematics with Georgia Southern University, Statesboro, GA, USA. His research interests include signal processing, image reconstruction, matrix theory, and numerical analysis.

FANGJUN ARROYO received the Ph.D. degree in mathematics from the Graduate Center, The City University of New York, New York, NY, USA, in 1992. She is currently a Professor of Mathematics with Francis Marion University, Florence, SC, USA. Her research interests include algebraic homotopy theory, combinatorics, and image processing algorithms.

JIEHUA ZHU received the Ph.D. degree in applied mathematical and computational sciences from the University of Iowa, Ames, IA, USA, in 2005. She is currently a Professor of Mathematics with Georgia Southern University, Statesboro, GA, USA. Her current research interests include biomedical imaging, computed tomography, and pattern recognition.

JIANING SUN received the Ph.D. degree in computational mathematics from the Mathematics School and the Institute of Jilin University, Jilin, China, in 2008. He is currently a Lecturer of Information and Computational Science with Northeast Normal University, Changchun, China. His current research interests include compressive sensing, convex and non-convex optimization, and imaging-based non-destructive testing techniques.